



# Numerical modeling of a rotary cement kiln with improvements to shell cooling



Christopher Csernyei, Anthony G. Straatman\*

Department of Mechanical & Materials Engineering, Western University, London, Ontario N6A 5B9, Canada

## ARTICLE INFO

### Article history:

Received 16 March 2016

Received in revised form 8 June 2016

Accepted 20 June 2016

### Keywords:

Convection

Numerical modeling

Rotary kiln

Cement

Kiln shell cooling

## ABSTRACT

Numerical models are developed by researchers to analyze and understand the trends occurring within rotary kilns, and allow for improvements in terms of energy quantification and usage. The present study develops a one-dimensional kiln model using elements of existing models and then links the model to the surroundings via a composite resistance model and a forced convection model that enables proper inclusion of the effects of shell-cooling fans. Shell-cooling fans are common in industry and allow for a reduction in shell temperature and promotion of internal coating formation. Thermal conductivity through the kiln shell is treated as a calibration parameter to allow for a more accurate shell temperature profile to be generated, while a forced convection model developed for a bank of jets impinging on a large cylinder is implemented to quantify the external convective resistance. The governing heat transfer and chemistry equations are implemented into the Matlab R2014a software to produce one-dimensional solutions of the temperature distributions and species mass fractions observed in a rotary cement kiln. A validation study is performed against an existing one-dimensional model showing reasonable quantitative and qualitative results of temperature profiles and species outputs. Using operational parameters from a partner organization, a profile of internal and external temperature profiles and the corresponding axial development of species products is also presented. Scanned shell temperature data is then compared against the results of the model considering only free convection, and forced convection from the kiln shell cooling fans in operation. An error of  $\geq 20\%$  was observed when the effects of forced convection on the kiln shell are neglected.

© 2016 Elsevier Ltd. All rights reserved.

## 1. Introduction

The goal in cement production is inherently to produce as much cement as possible while consuming the least amount of energy possible. Measurements of energy consumption at a cement plant, and within the cement industry as a whole, are typically expressed as energy/weight of clinker, which is the fundamental building block of the process. Rotary cement kilns are used for the production of cement clinker and are by far the highest consumer of thermal energy in the operation, requiring a continuous input of fuel to facilitate the chemical reactions necessary for clinker production. Not surprisingly, 30–40% of the heat released from a cement plant is from the kiln as a by-product of the clinker production process [1,2]. With such large amounts of heat being input, consumed, and generated within the rotary kiln, there is also a large amount of heat released from the kiln. Engin and Vedat [3] performed a case study on heat recovery for dry-type cement rotary kiln systems and observed that approximately 40% of the total input

energy to the kiln was released in the form of hot flue gas (19.15%), cooler stack emissions (5.61%), and via convection and radiation from the kiln shell (15.11%). From these releases, the hot flue gas is typically reused throughout the plant in preheating and drying operations; however, the cooler stack emissions and all of the heat released from the kiln shell due to radiation and convection are lost to the surroundings. Thus, the rotary kiln is the largest source of waste heat in the plant, and this has prompted researchers to conduct analyses on the rotary cement kiln through the use of one-dimensional mathematical models and three-dimensional CFD simulations.

At its core, the rotary cement kiln is a large chemical reactor; a simple schematic of the layout of a rotary cement kiln is shown in Fig. 1. Tilted at an angle of 2–5° with respect to horizontal, and operating at a slow rotating speed of approximately 1–5 rpm, the raw feed (typically limestone, silica, aluminum and iron oxide, [4]) enters at the elevated end, and travels through the cylindrical kiln due to gravity/tumbling. The kiln is comprised of a steel shell for strength and rigidity, lined on the inner surface with refractory brick to enhance the thermal resistance, and to isolate the steel shell from the high temperature process taking place inside. Raw

\* Corresponding author.

E-mail address: [astraatman@eng.uwo.ca](mailto:astraatman@eng.uwo.ca) (A.G. Straatman).

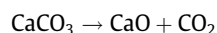
## Nomenclature

$A_{rgb}$	radiation area internal gas to bulk bed [m]	$Q_{stl}$	heat transfer through steel shell [W/m]
$A_{rgw}$	radiation area internal gas to internal wall [m]	$Q_{conv-shell}$	heat transfer from shell by convection [W/m]
$A_{rwb}$	radiation area internal wall to bed [m]	$Q_{rad-shell}$	heat transfer from shell by radiation [W/m]
$A_{cgb}$	convection area internal gas to bulk bed [m]	$Ra_D$	Rayleigh number
$A_{cgw}$	convection area internal gas to internal wall [m]	$Re_d$	jet Reynolds number
$A_{cwb}$	conduction area internal wall to bed [m]	$Re_D$	axial Reynolds number
$A_{segment}$	area of bed segment [m]	$Re_w$	angular Reynolds number
$A_{sh}$	area of steel shell [m]	$R_g$	universal gas constant [J/mol K]
$A_j$	pre-exponential factor for jth reaction [1/s]	$R$	internal radius of kiln [m]
$A_i$	initial value of $Al_2O_3$ at input	$Si$	initial value of $SiO_2$ at input
$Cp_b$	specific heat of bulk bed [J/kg K]	$SC_{CO_2}$	source term for heat release from $CO_2$ [W/m]
$C_{Tmax}$	maximum coating thickness [m]	$T_g$	freeboard gas temperature [K]
$D_e$	hydraulic diameter of kiln [m]	$T_b$	bulk bed temperature [K]
$D$	diameter of kiln [m]	$T_w$	internal wall temperature [K]
$E_j$	activation energy for jth reaction [J/mol]	$T_0$	temperature of atmosphere [K]
$Fi$	initial value of $Fe_2O_3$ at input	$T_{sh}$	temperature of steel shell [K]
$\Delta H_{CaCO_3}$	heat of reaction $CaCO_3$ [J/kg]	$u_g$	airspeed of freeboard gas [m/s]
$\Delta H_{C_2S}$	heat of reaction $C_2S$ [J/kg]	$v_b$	velocity of bulk bed [m/s]
$\Delta H_{C_3S}$	heat of reaction $C_3S$ [J/kg]	$Y_n$	mass fraction of nth species
$\Delta H_{C_3A}$	heat of reaction $C_3A$ [J/kg]	$Y_{fus}$	fusion fraction
$\Delta H_{C_4AF}$	heat of reaction $C_4AF$ [J/kg]	$d/D$	ratio of jet diameter to cylinder diameter
$h_{cgb}$	convective heat transfer coefficient freeboard gas to bulk bed [W/m <sup>2</sup> K]	$y/d$	jet-to-cylinder spacing
$h_{cgw}$	convective heat transfer coefficient freeboard gas to internal wall [W/m <sup>2</sup> K]	$z/d$	jet-to-jet spacing
$h_{cwb}$	coefficient for conduction from wall to bed [W/m <sup>2</sup> K]	$x/d$	Jet offset from centerline
$h_{csh}$	convective heat transfer coefficient from shell to atmosphere [W/m <sup>2</sup> K]		
$k_g$	thermal conductivity of freeboard gas [W/m K]		
$k_b$	thermal conductivity of bulk bed [W/m K]	<i>Greek characters</i>	
$k_a$	thermal conductivity of air [W/m K]	$\alpha_b$	bulk bed thermal diffusivity [m <sup>2</sup> /s]
$k_1$	reaction rate $CaCO_3$ [1/s]	$\alpha_g$	absorptivity of freeboard gas
$k_2$	reaction rate $C_2S$ [1/s]	$\beta$	angle of repose [rad]
$k_3$	reaction rate $C_3S$ [1/s]	$\varepsilon_{sh}$	emissivity of steel shell
$k_4$	reaction rate $C_3A$ [1/s]	$\varepsilon_g$	emissivity of freeboard gas
$k_5$	reaction rate $C_4AF$ [1/s]	$\varepsilon_b$	emissivity of bulk bed
$L_{fus}$	latent heat of fusion [J/kg]	$\varepsilon_w$	emissivity of internal wall
$L_{gcl}$	chord length of bed segment [m]	$\Gamma$	angle of fill of kiln [rad]
$\dot{m}_{CO_2}$	mass flow rate of $CO_2$ [kg/s]	$\mu_g$	dynamic viscosity of freeboard gas [s/m <sup>2</sup> ]
$\dot{m}_{CaCO_3}$	mass flow rate of $CaCO_3$ [kg/s]	$\eta$	degree of solid fill
$M_n$	molar mass of nth species [kg/kmol]	$\omega$	rotational speed of kiln [rad/s]
$Nu_{ave}$	average Nusselt number for forced convection from cylinder	$\Omega$	view factor for radiation
$Pr$	Prandtl number	$\rho_g$	density of freeboard gas [kg/m <sup>3</sup> ]
$Q_{rgb}$	radiation heat transfer gas to bulk bed [W/m]	$\rho_s$	density of solids [kg/m <sup>3</sup> ]
$Q_{rgw}$	radiation heat transfer gas to internal wall [W/m]	$\sigma$	Stefan–Boltzmann constant
$Q_{rwb}$	radiation heat transfer internal wall to bed [W/m]	$v_g$	kinematic viscosity of freeboard gas [m <sup>2</sup> /s]
$Q_{cgb}$	convection heat transfer gas to bulk bed [W/m]		
$Q_{cgw}$	convection heat transfer gas to internal wall [W/m]	<i>Species</i>	$CaCO_3$
$Q_{cwb}$	conduction heat transfer internal wall to bed [W/m]		$SiO_2$
$Q'$	heat gained by bed due to heat transfer [W/m]		$CaO$
$q_c$	heat generated by chemical reactions [W/m <sup>3</sup> ]		$Fe_2O_3$
$Q_{coat}$	heat transfer through coating [W/m]		$Al_2O_3$
$Q_{ref}$	heat transfer through refractory [W/m]		$C_2S$
			$C_3S$
			$C_3A$
			$C_4AF$

feed enters the kiln at one end, and the fuel (petroleum coke which is combusted in a burner located approximately 1 m into the kiln) enters at the opposite end. There are four main regions within the rotary kiln [5] (refer to Fig. 1a):

- Preheating/drying: The initial region of the kiln is where raw material is dried and all remaining moisture is evaporated out of the mixture. The temperature of the raw material increases to approximately 1173 K (900 °C) where calcination can begin.

- Calcining/decomposition: Calcination occurs in this region, indicating that the limestone,  $CaCO_3$ , will decompose into calcium oxide (free lime),  $CaO$  and carbon dioxide:



This is one of the most important stages in the cement production process, as limestone that is not properly calcined will be difficult to burn, and can result in a poor quality product.

Download English Version:

<https://daneshyari.com/en/article/7055181>

Download Persian Version:

<https://daneshyari.com/article/7055181>

[Daneshyari.com](https://daneshyari.com)